

On the Adversarial Robustness of Learning-based Image Compression Against Rate-Distortion Attacks

Chenhao Wu, Qingbo Wu, *Member, IEEE*, Haoran Wei, Shuai Chen, Lei Wang, King Ngi Ngan, *Fellow, IEEE*, Fanman Meng, *Member, IEEE*, Hongliang Li, *Senior Member, IEEE*

Abstract—Despite demonstrating superior rate-distortion (RD) performance, learning-based image compression (LIC) algorithms have been found to be vulnerable to malicious perturbations in recent studies. Adversarial samples in these studies are designed to attack only one dimension of either bitrate or distortion, targeting a submodel with a specific compression ratio. However, adversaries in real-world scenarios are neither confined to singular dimensional attacks nor always have control over compression ratios. This variability highlights the inadequacy of existing research in comprehensively assessing the adversarial robustness of LIC algorithms in practical applications. To tackle this issue, this paper presents two joint rate-distortion attack paradigms at both submodel and algorithm levels, *i.e.*, Specific-ratio Rate-Distortion Attack (SRDA) and Agnostic-ratio Rate-Distortion Attack (ARDA). Additionally, a suite of multi-granularity assessment tools is introduced to evaluate the attack results from various perspectives. On this basis, extensive experiments on eight prominent LIC algorithms are conducted to offer a thorough analysis of their inherent vulnerabilities. Furthermore, we explore the efficacy of two defense techniques in improving the performance under joint rate-distortion attacks. The findings from these experiments can provide a valuable reference for the development of compression algorithms with enhanced adversarial robustness.

Index Terms—Robust image compression, rate-distortion attack, adversarial examples

I. INTRODUCTION

IMAGE compression is a fundamental task in the field of image processing and has been extensively studied over the past few decades. Generations of traditional handcrafted codecs have facilitated the image storage and transmission, *e.g.*, JPEG [1], HEVC [2], and VVC [3]. In recent years, there has been a growing interest within the image processing community towards learning-based image compression (LIC), which achieves superior rate-distortion (RD) performance with end-to-end optimized models [4]–[6].

Although learning-based image compression methods have demonstrated significant potential in practical applications within real-world scenarios, it is essential for them to undergo rigorous verification on the robustness. One of the most severe challenges in this regard is the security against adversarial attacks, commonly known as adversarial robustness. This

The Authors are with the School of Information and Communication Engineering, University of Electronic Science and Technology of China, Chengdu, 611731, China (e-mail: chwu@std.uestc.edu.cn; qbwu@uestc.edu.cn; hrwei@std.uestc.edu.cn; schen@std.uestc.edu.cn; lwang@std.uestc.edu.cn; knngan@uestc.edu.cn; hlli@uestc.edu.cn; fmmeng@uestc.edu.cn)

Corresponding author: Qingbo Wu.

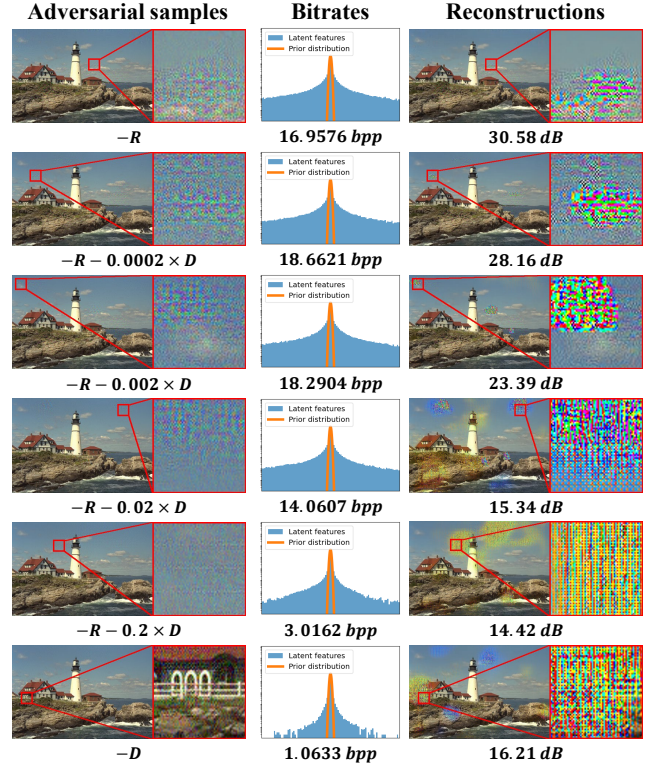


Fig. 1. Visualization of input images and compression results of *Minnen2018 submodel-5* under different attack directions.

means defending against the malicious samples generated from adversaries who attack the compression system [7].

Recently, several works [8]–[10] have explored the vulnerability of the learning-based image compression to adversarial attacks concerning either bitrate or distortion in a singular dimension. By applying malicious perturbations to input image, adversaries can induce the compression model to produce corrupted reconstruction [8], [9] or significant increase in bitrate [10]. This observation confirms the susceptibility of LIC to adversarial attacks. However, a simplistic unidimensional attack falls short in providing a comprehensive investigation on the adversarial robustness of the LIC algorithm. In real-world scenarios, attacks may arise from arbitrary combinations of bitrate attack and distortion attack, leading to diverse impacts on compression and reconstruction results, as shown in Fig. 1. Another characteristic of typical compression scenarios is the implementation of rate control, which is based upon limited storage size or communication bandwidth [11], [12].

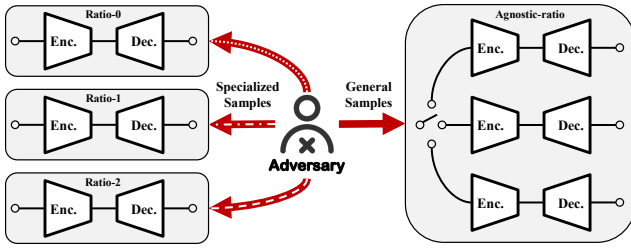


Fig. 2. **Left:** Specific-ratio Rate-Distortion Attack (SRDA), where adversarial samples are designed for specific compression ratios. **Right:** Agnostic-ratio Rate-Distortion Attack (ARDA), which seeks to attack all compression ratios with general adversarial samples.

This renders the unpredictable effects of adversarial examples designed for submodels of specific compression ratios.

Drawing from the observations of practical scenarios, this paper formulates two attack paradigms: the Specific-ratio Rate-Distortion Attack (SRDA) and the Agnostic-ratio Rate-Distortion Attack (ARDA), as illustrated in Fig. 2. Specifically, SRDA generates dedicated adversarial samples for submodels at specific compression ratios, while ARDA destructs the entire compression algorithm at all ratios with a single malicious image. In both paradigms, adversaries maintain the flexibility to degrade the compression performance in arbitrary directions within the RD plane.

To assess the adversarial robustness of the LIC algorithm against malicious attacks, this paper introduces a suite of multi-granularity assessment tools. Specifically, we utilize the variation in RD performance as the global metric and employ local attack effects, including patch-wise bitrate analysis and pixel-wise distortion analysis, as local metrics. These metrics can offer a comprehensive understanding of adversarial robustness through algorithm-level, submodel-level, and image-level analysis.

By employing the attack paradigms and assessment tools outlined in this paper, we conducted a comprehensive investigation into the adversarial robustness of eight representative LIC algorithms. Additionally, we examined the effectiveness of two defense techniques: adversarial training and online updating. The former involves finetuning LIC models with adversarial samples generated by SRDA, while the latter optimizes the compression results online in the opposite direction with attacks. Experimental results comprehensively reveal the characteristics of the LIC algorithm under malicious attacks in practical scenarios and assess the efficacy of defense techniques in enhancing the robustness. These findings provide a sufficient reference for the advancement of learning-based compression methods with improved adversarial robustness.

II. RELATED WORK

A. Learning-based Image Compression

Prototype models of the prevailing autoencoder-type image compression were initially proposed and developed in [13] and [14], with the factorized prior model and hyperprior model still playing crucial roles in state-of-the-art approaches. In [4] and [5], context information was extracted from the decoded

latent features through masked convolutional layers to improve the modeling of prior distribution. To improve the spatial modeling capability, [6] and [15] adopted the structure of transformer to better capture the local and global information. These algorithms rely on separately trained submodels for each bitrate, in contrast, [16] and [17] adopted the variable-rate design, achieving multiple compression ratios using a single model.

B. Attack and Defense

Deep learning models have been observed to be vulnerable under adversarial attacks [18], which are typically executed by introducing imperceptible disturbances to the regular input. To evaluate the adversarial robustness of neural networks, many adversarial attack algorithms have been designed to generate malicious adversarial samples [19]–[22].

Recently, the vulnerability of individual submodels in LIC algorithms has been investigated concentrating on a singular dimension of either bitrate or distortion. To assess the distortion vulnerability, [8] developed a fast threshold-constrained distortion attack method, while [9] mitigated the perceptibility of the malicious disturbance by imposing constraints on low frequencies. To examine the bitrate vulnerability, [10] raised the bitrate using malicious perturbations while maintaining reconstruction quality.

III. PRELIMINARY

Learning-based image compression model usually contains an image encoder $g_a(\cdot)$ for feature extraction and an image decoder $g_s(\cdot)$ for reconstruction, together with an entropy model for losslessly encoding quantized features. When compressing, the input image x is first transformed to latent representation $y = g_a(x)$, and then quantized to $\hat{y} = Q(y)$ to execute entropy encoding. Inversely, \hat{y} is entropy decoded and transformed back to reconstructed image $\hat{x} = g_s(\hat{y})$. During training, the loss function is usually defined as a trade-off between the bitrate $\mathcal{R}(x)$ consumed by compressed binary strings and the distortion $\mathcal{D}(x)$ in decoded images, which can be formulated as the rate-distortion loss:

$$\mathcal{L}_{rd} = \mathcal{R}(x) + \lambda \mathcal{D}(x), \quad (1)$$

where λ is the trade-off factor that controls the balance between two loss items.

Adversarial examples are often defined as inputs that are designed to cause the model to make mistakes [23]. Given an input image x , it can be modified to x_a by adding malicious noise δ :

$$x_a = x + \delta, \quad \|\delta\| \leq \epsilon, \quad x_a \in [0, 1]. \quad (2)$$

ϵ is the maximum level of disturbance, $\|\cdot\|$ is defined as the averaged l_2 -norm in this paper. By intentionally designing the perturbation δ , it is expected that the RD performance on the input x_a will exhibit significant degradation compared to the original input x . Since most image compression algorithms used in practical applications are standardized, researches on adversarial robustness are often conducted within the context of white-box attacks [8], [9].

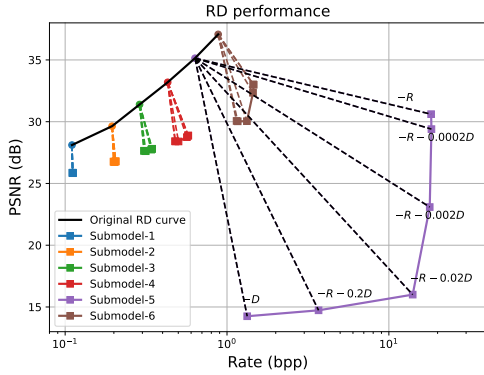


Fig. 3. RD performance of Minnen2018 on adversarial images specifically designed for submodel-5.

IV. ATTACK PARADIGMS

A. Specific-ratio Rate-Distortion Attack

When the compression ratio to be used by the target LIC algorithm can be determined by the adversaries, the specially crafted adversarial samples can exert maximum effect. In response to this situation, we developed the Specific-ratio Rate-Distortion Attack (SRDA) to carry out attacks in various directions. The perturbation δ can be inferred by optimizing Eq. (3) under the constraint of Eq. (2):

$$\arg \min_{\delta} \mathcal{L}_s = -\gamma_r \cdot \mathcal{R}(x_a) - \gamma_d \cdot \mathcal{D}(x_a), \quad (3)$$

where γ_r and γ_d are attack coefficients controlled by adversaries. When γ_r and γ_d are set to 0 and 1, adversarial samples are crafted to increase reconstruction distortion, as considered in [8] and [9]. When γ_r is set to 1 and γ_d is set to a negative value, it turns into the bitrate attack without compromising reconstruction quality in [10].

We primarily investigate six attack directions, where (γ_r, γ_d) are set to $(1, 0)$, $(1, 0.0002)$, $(1, 0.002)$, $(1, 0.02)$, $(1, 0.2)$, and $(0, 1)$, respectively. Given the high correlation among similar attack directions, we can utilize the results from these six directions to estimate unexplored performance. The implementation of SRDA follows a similar practice to [8], the difference is that we control the number of attack steps after the perturbation reaching the surface of ϵ -sphere for fairness. Take submodel-5 of Minnen2018 [4] as an example, we show the RD performance before and after SRDA in Fig. 3 purple lines. The significant variation in RD performance across different attack directions is evident.

B. Agnostic-ratio Rate-Distortion Attack

However, when the compression ratio to be used by the target LIC algorithm can not be determined by the adversaries, the efficacy of specially crafted adversarial samples can not be guaranteed. As shown in Fig. 3, the efficacy of adversarial samples specially designed for submodel-5 exhibits a notable decrease when compressed by other submodels.

To ensure the effectiveness of malicious attacks, adversaries need to design adversarial samples targeting a broader range of

Algorithm 1 Specific-ratio Rate-Distortion Attack (SRDA)

Input: Image $x \in \mathbb{R}^{H \times W \times C}$, attack coefficients γ_r and γ_d , maximum disturbance ϵ , attack steps \mathcal{T} on the surface of ϵ -sphere.

1: **Initialization:** $\delta = \vec{0}^{H \times W \times C}$

2: **repeat**

3: **while** $\|\delta\| > \epsilon$ **do**

4: $\arg \min_{\delta} \|\delta\|$

5: **end while**

6: Calculate \mathcal{L}_s based on γ_r and γ_d . ▷ Eq. (3)

7: Update δ based on $\partial \mathcal{L}_s / \partial \delta$.

8: **until** \mathcal{T} attacks are made after the first reach of the ϵ -sphere surface

Output: $\max(\min(x_a, 1), 0)$

bitrates. This Agnostic-ratio Rate-Distortion Attack (ARDA) can be extended from SRDA as follows:

$$\arg \min_{\delta} \mathcal{L}_f = \sum_{k=1}^N w^{(k)} \mathcal{L}_s^{(k)}, \quad (4)$$

where N is the number of submodels to attack, k indicates the index of submodel, $\mathcal{L}_s^{(k)}$ represents the \mathcal{L}_s of SRDA on submodel k , $w^{(k)}$ is the weight used to balance the attack effect on submodel- k with $\sum_{k=1}^N w^{(k)} = 1$.

Given the inconsistent adversarial robustness among submodels, employing identical weights could lead to the concentration of attack impacts on specific bitrates. To mitigate this issue and distribute the attack effects evenly across all bitrates, we dynamically adjust the weights based on the observed attack effects throughout the attack procedure:

$$w^{(k)} = \frac{\exp(w^{(k)}/\tau)}{\sum_i \exp(w^{(i)}/\tau)}, \quad w^{(k)} = \mathcal{L}_{s-init}^{(k)} / \mathcal{L}_s^{(k)}, \quad (5)$$

where τ is the temperature coefficient that controls the difference among $w^{(k)}$.

V. MULTI-GRANULARITY ASSESSMENT TOOLS

In this section, a suite of multi-granularity assessment tools is developed to evaluate and analyse the adversarial robustness of LIC methods. Based on the compression results of the original image and the maliciously perturbed image, the variation in RD performance can be calculated as:

$$\Delta \mathcal{R} = \mathcal{R}(x_a) - \mathcal{R}(x), \quad \Delta \mathcal{D} = \mathcal{D}(x_a) - \mathcal{D}(x). \quad (6)$$

With this variation as global metric, we can intuitively compare the adversarial robustness of various algorithms and submodels.

For a finer analysis, we further introduce the local attack effects, including patch-wise bitrate analysis and pixel-wise distortion analysis:

$$\Delta_s \mathcal{R} = \mathcal{R}_s(y_a) - \mathcal{R}_s(y), \quad \Delta_s \mathcal{D} = \mathcal{D}_s(x_a) - \mathcal{D}_s(x), \quad (7)$$

where the subscript s indicates that the spatial information is retained during the calculation of performance. On this basis,

the local attack success ratios on bitrate and distortion can be calculated as:

$$\mathcal{S}_{\mathcal{R}} = \frac{\sum \mathbb{I}(\Delta_s \mathcal{R} > \mathcal{R}_T)}{N_{\mathcal{R}}}, \quad \mathcal{S}_{\mathcal{D}} = \frac{\sum \mathbb{I}(\Delta_s \mathcal{D} > \mathcal{D}_T)}{N_{\mathcal{D}}}, \quad (8)$$

where $\mathbb{I}(\cdot)$ denotes the indicator function, which is 1 when the condition inside it holds true. \mathcal{R}_T and \mathcal{D}_T are the thresholds of success attacks. $N_{\mathcal{R}}$ and $N_{\mathcal{D}}$ are the total numbers of elements in $\Delta_s \mathcal{R}$ and $\Delta_s \mathcal{D}$, respectively.

VI. DEFENSE TECHNIQUES

A. Adversarial Training

Adversarial training (AT) is one of the most effective defense methods against attacks of known types [24]. Its fundamental concept is to improve the adversarial robustness of learning-based models by training them with adversarial samples. Consequently, the essence of this method lies in achieving comprehensive coverage of the adversarial example space. To effectively counter attacks from arbitrary directions and encompass a wide array of malicious images, we generate adversarial samples by randomly adjusting attack coefficients γ_r and γ_d of SRDA.

B. Online Updating

Online updating, initially introduced in [25], stands as a content-adaptive optimization technology. Due to the common practice of training LIC algorithms on a vast dataset of images, the resulting model often yields compromised RD performance across all training images. To adapt effectively to a specific input image, online updating iteratively adjusts the latent features to minimize the RD loss as defined in Eq. (1).

Disregarding the influence of trade-off factors, its objective stands in opposition to the goals of adversarial attacks, rendering it inherently applicable as a defense technology. In defense, we directly update input image x_a to keep consistent with the attacks. This technique does not need an additional training process but requires multiple iterations of encoding.

VII. EXPERIMENTS AND FINDINGS

A. Settings

1) *Models*: We conduct experiments on Ballé2016¹ [13], Ballé2018¹ [14], Minnen2018¹ [4], Cheng2020¹ (self-attention variant) [5], Song2021² [16], Cai2022³ [17], Zou 2022⁴ [6] and Liu2023⁵ [15] based on CompressAI platform [26]. These methods encompass various important structures in the field of image compression and are highly representative. Key components of each method are shown in Tab. I. A submodel with fixed compression ratio is designed for each bitrate in separately trained methods. For a fair comparison, 6 submodels under 1.0 *bpp* are selected for the evaluation of robustness against ARDA. In variable-rate methods, a set of

base parameters is shared by all bitrates. In order to compare with separately trained algorithms, we set the quality level of variable-rate methods to 10, 25, 40, 55, 70, 90 as the six submodels.

2) *Datasets*: Evaluation of the attack and defense is performed on Kodak dataset [27], which contains 24 full color images with resolution 512×768 . Adversarial training is performed on 14500 pictures with resolution around 1024×1024 from the web. The training images are preprocessed to remove undesirable artifacts following [14].

3) *Attack*: All the attack is conducted with *Adam* optimizer with learning rate of 10^{-2} , which is decreased to 10^{-3} when attacking $\mathcal{T}/2$ steps on the surface of ϵ -sphere. The total step of adversarial attack \mathcal{T} is set to 64 by default, ϵ is set to 10^{-3} in all experiments. Temperature coefficient τ in the weight of ARDA is set equal to γ .

4) *Defense*: In adversarial training, training images are randomly cropped to 256×256 . On the basis of normally trained models, the compression models to be protected is optimized on both normal and perturbed images by *Adam* for 1000 iterations. The learning rate is initialized to 10^{-4} and decreased to 10^{-5} during the last 10% of training steps. In online updating, the learning rate is set to 10^{-2} .

B. Comparison of Adversarial Robustness

Following the conventional practice in the image compression literature, we present the performance of all comparative methods under the same attack under SRDA within the RD plane, as shown in Fig. 4. Differently, RD performance on original images and the maliciously perturbed images is presented in the same plot for direct comparison. Dashed lines are utilized to connect RD points across different submodels, as there is a lack of specific correlation between their performance.

1) *Overall Adversarial Robustness*: Based on the compression results before and after malicious attacks, we conduct the algorithmic level statistical analysis to evaluate the adversarial robustness of LIC methods utilizing Eq. (6). The averaged performance variations $\mu(\Delta \mathcal{R})$ and $\mu(\Delta \mathcal{D})$ can be calculated by averaging across all the submodels of a specific LIC method. By further averaging them across six attack directions to $\bar{\mu}(\Delta \mathcal{R})$ and $\bar{\mu}(\Delta \mathcal{D})$, we can obtain the overall adversarial robustness in Tab. II.

The performance of all compression algorithms significantly degrades under SRDA. When comparing from a single dimension, bitrate of Ballé2016 and distortion of Zou2022 exhibit the best adversarial robustness among them. However, the other dimension of them, *i.e.*, distortion of Ballé2016 and bitrate of Zou2022, demonstrate the worst robustness. Taking both dimensions into account, Ballé2018 and Cheng2020 demonstrate superior adversarial robustness by achieving relatively low values in both bitrate and distortion.

Compared to SRDA, most algorithms demonstrate notably better adversarial robustness against ARDA. This suggests that the adaptive rate control can reduce the overall vulnerability of LIC algorithms by leveraging distinctions among submodels. Nevertheless, variable-rate methods Song2021 and Cai2022

¹<https://github.com/InterDigitalInc/CompressAI>

²<https://github.com/micmic123/QmapCompression>

³<https://github.com/CaiShilv/HiFi-VRIC>

⁴<https://github.com/Googolxx/STF>

⁵https://github.com/jmliu206/LIC_TCM

TABLE I

KEY COMPONENTS OF VICTIM MODELS. *SFT* AND *INN* ARE SPATIAL FEATURE TRANSFORM AND INVERTIBLE NEURAL NETWORK. *(S)W-MSA*, *LN*, AND *MLP* STAND FOR (SHIFTED) WINDOW-BASED MULTI-HEAD SELF-ATTENTION, LAYER NORMALIZATION, AND MULTILAYER PERCEPTRON. *GDN* MEANS GENERALIZED DIVISIVE NORMALIZATION.

	Structure Type	Transform Coding Layers	Entropy Model	Method Type
Ballé2016 [13]	CNN-based	Conv. + GDN	Factorized	Separately
Ballé2018 [14]	CNN-based	Conv. + GDN	Hyperprior	Separately
Minnen2018 [4]	CNN-based	Conv. + GDN	Hyperprior & Spatial context	Separately
Cheng2020 [5]	CNN-based	Conv. + Res. + Attn. + GDN	Hyperprior & Spatial context	Separately
Song2021 [16]	CNN-based	Conv. + Res. + SFT + GDN	Hyperprior	Variable-rate
Cai2022 [17]	Mixed INN-CNN	Conv. + Dense. + INN + SFT + GDN	Hyperprior & Spatial context	Variable-rate
Zou2022 [6]	Transformer-based	(S)W-MSA + LN + MLP	Hyperprior & Channel context	Separately
Liu2023 [15]	Mixed Transformer-CNN	Conv. + Res. + (S)W-MSA + LN + MLP + GDN	Hyperprior & Channel context	Separately

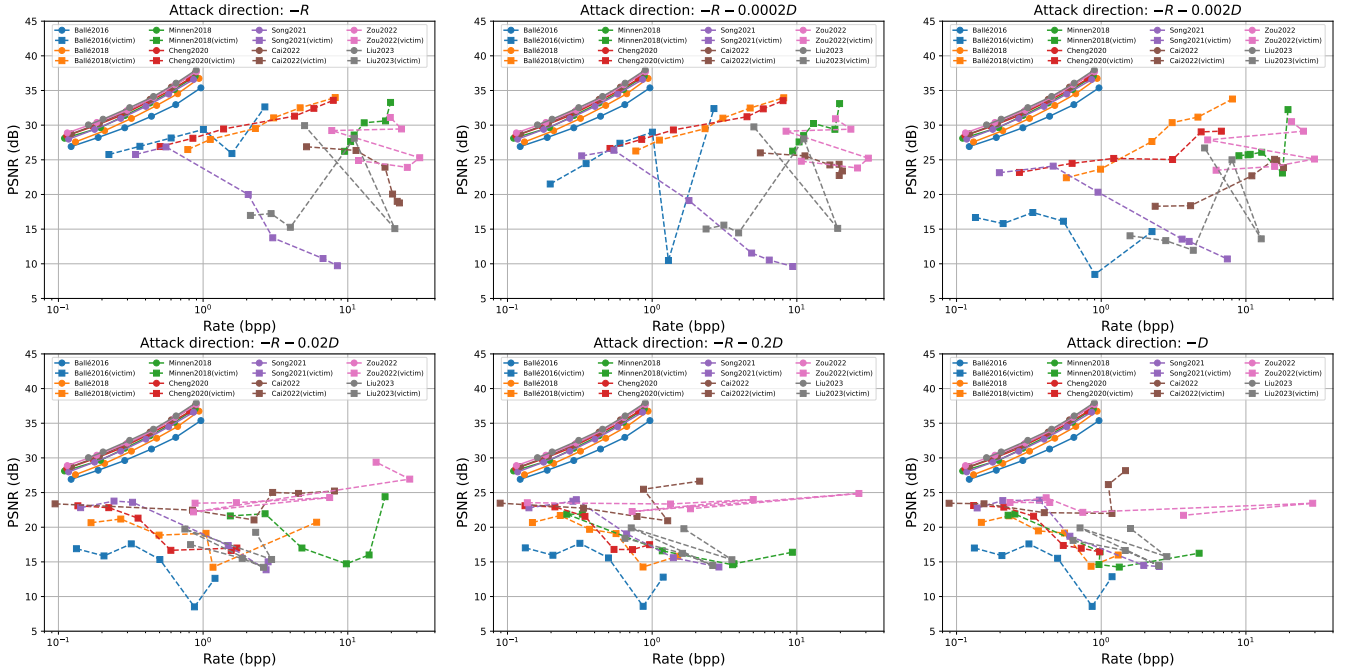


Fig. 4. RD performance under six attack directions of SRDA. The performance of the same compression algorithm before and after an attack is depicted using solid and dashed lines in the same color.

exhibit weaker adversarial robustness when compared to separately trained methods. This observation indicates that the utilization of a shared set of base parameters will result in similar vulnerabilities across submodels.

2) Adversarial Robustness in Different Attack Directions:

In order to gain deeper insights into the robustness of the LIC algorithm across various attack directions, we present the averaged performance variations $\mu(\Delta\mathcal{R})$ and $\mu(\Delta\mathcal{D})$ in Figs. 5 and 6.

As observed in Fig. 5, the values of $\mu(\Delta\mathcal{R})$ and $\mu(\Delta\mathcal{D})$ for Ballé2018, Minnen2018, and Cheng2020 exhibit gradual decreases and increases, respectively, as the attack direction shifts from bitrate attack to distortion attack. This findings suggest that their vulnerabilities are evenly distributed in terms of bitrate and distortion. Differently, $\mu(\Delta\mathcal{D})$ of Cai2022 and Zou2022, as well as $\mu(\Delta\mathcal{R})$ of Ballé2016, demonstrate negligible variations with shifts in attack direction and consistently remain at relatively low levels. This indicates that their vulnerability is mainly confined to a singular dimension.

In contrast to the aforementioned patterns, the values of

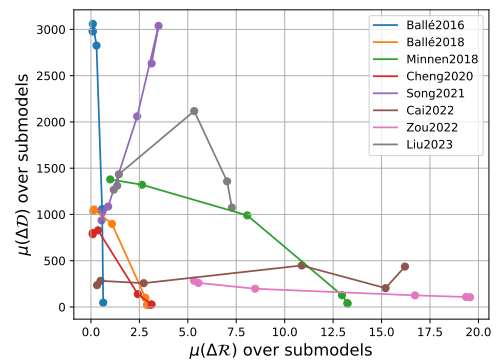


Fig. 5. Averaged performance variations over all submodels under six attack directions of SRDA.

$\mu(\Delta\mathcal{D})$ of Song2021 and Liu2023 show an abnormal increase with the strengthening of bitrate attacks. Additionally, these values are markedly high when subjected to singular dimen-

TABLE II
 AVERAGED PERFORMANCE VARIATIONS (\downarrow) OVER ALL SUBMODELS AND ATTACK DIRECTIONS. THE BEST AND WORST ADVERSARIAL ROBUSTNESS AMONG ALL METHODS ARE HIGHLIGHTED IN BLUE AND RED.

Methods	SRDA				ARDA			
	$\bar{\mu}(\Delta\mathcal{R})$	$\bar{\mu}(\Delta\mathcal{D})$	$\bar{\sigma}(\Delta\mathcal{R})$	$\bar{\sigma}(\Delta\mathcal{D})$	$\bar{\mu}(\Delta\mathcal{R})$	$\bar{\mu}(\Delta\mathcal{D})$	$\bar{\sigma}(\Delta\mathcal{R})$	$\bar{\sigma}(\Delta\mathcal{D})$
Ballé2016 [13]	0.2974	2158.45	0.3051	2240.76	0.2113	119.35	0.1934	59.85
Ballé2018 [14]	1.6635	521.69	1.4792	379.95	0.4703	79.17	0.3685	46.54
Minnen2018 [4]	8.5247	649.08	3.5128	403.64	1.1586	72.35	0.8140	40.53
Cheng2020 [5]	1.5294	434.28	1.2946	268.29	0.4964	96.02	0.3436	40.94
Song2021 [16]	1.8357	1796.32	1.7483	1712.94	0.7213	194.10	0.7324	208.74
Cai2022 [17]	7.6381	310.75	3.3936	178.19	5.2461	137.18	0.9778	58.29
Zou2022 [6]	12.4988	180.11	9.0529	72.33	1.4290	75.74	1.8928	44.20
Liu2023 [15]	3.9357	1426.99	3.0803	839.32	0.4598	140.42	0.3537	61.99

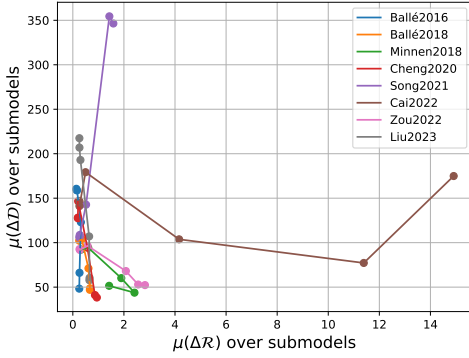


Fig. 6. Averaged performance variations over all submodels under six attack directions of ARDA.

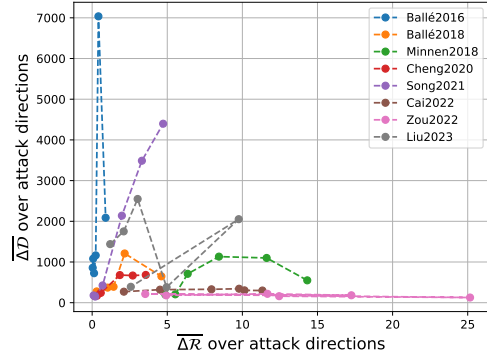


Fig. 7. Submodel-level averaged performance variations over all attack directions of SRDA.

sion attacks on bitrate. This phenomenon may result from the significant entanglement between the vulnerabilities in two dimensions, where an attack on one dimension could impact the other. The combination of attacks in both dimensions brings to a higher attack effects.

As observed in Fig. 6, the anomalous rise observed in Liu2023 has disappeared. This indicates that the entangled vulnerability exploited by SRDA is not universal across all submodels, and thus cannot be utilized in ARDA to attack all bitrates. In contrast, the entanglement within Song2021 persists, this can also be attributed to the base parameters shared between different submodels.

3) *Adversarial Robustness of Submodels*: To analyze the dispersion of individual submodels within the overall performance of the algorithm, we calculate the averaged standard deviations $\bar{\sigma}(\Delta\mathcal{R})$ and $\bar{\sigma}(\Delta\mathcal{D})$, as shown in Tab. II. In the meantime, we present the submodel-level averaged performance variations $\overline{\Delta\mathcal{R}}$ and $\overline{\Delta\mathcal{D}}$ across six attack directions of SRDA and ARDA in Figs. 7 and 8.

From the data of SRDA in Tab. II, even the adversarial robustness of submodels within the same LIC algorithm shows significant variability. Among them, $\Delta\mathcal{D}$ of Ballé2016 and $\Delta\mathcal{R}$ of Zou2022 exhibit the largest standard deviation. From Fig. 7, it can be noted that submodels of the same algorithm tend to emphasize similar vulnerability dimensions, although the degree of robustness is varying. This suggests that the architecture of the network plays an important role in deter-

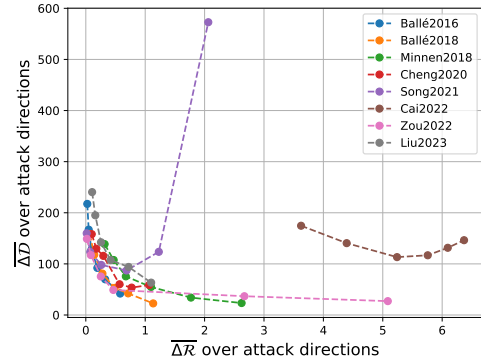


Fig. 8. Submodel-level averaged performance variations over all attack directions of ARDA.

mining the vulnerable attack directions, while factors during training like target bitrate and randomly sampled training images mainly impact the level of robustness.

From the data of ARDA in Tab. II and Fig. 8, the introduction of general adversarial samples increases the consistency among the robustness of submodels. Nonetheless, certain submodels in Song2021 and Zou2022 still exhibit considerable deviations, suggesting a higher vulnerability than others submodels to universal malicious disturbances.

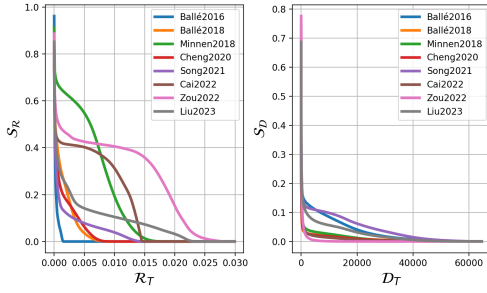


Fig. 9. Local attack success ratios over all submodels and all attack directions of SRDA.

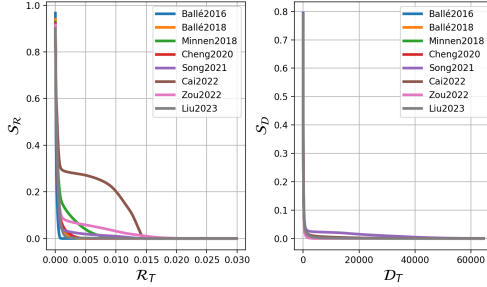


Fig. 10. Local attack success ratios over all submodels and all attack directions of ARDA.

C. Comparison of Local Attack Effects

Following the definition of local attack success ratios in Eq. (8), we can get the algorithmic level local analysis under SRDA and ARDA in Figs. 9 and 10 by adjusting thresholds \mathcal{R}_T and \mathcal{D}_T . It is evident that different LIC algorithms exhibit different performance degradation patterns. For instance, Minnen2018 exhibits a tendency to increase the bitrate slightly across a large number of patches, while Zou2022 increases the bitrate substantially at fewer positions. Likewise, the reconstruction of Song2021 is more vulnerable to be attacked compared to other algorithms under the SRDA when evaluated with a large \mathcal{D}_T .

In addition, the local attack effects can be utilized to analyze the reconstructions at the image-level. For instance, we visualize the decoded results of Ballé2016 and Song2021 in Fig. 11, and mask out the areas of successful and unsuccessful attacks by setting the threshold \mathcal{D}_T to 500. It is evident that the reconstructions of both algorithms will be significantly disrupted under SRDA. While under ARDA, this disruption is largely suppressed, only the common vulnerable regions shared by all submodels in SRDA retain. However, by comparing the two algorithms, the disrupted regions in submodels of Ballé2016 exhibit significant discrepancies, leading to a small fraction of regions being effectively attacked by ARDA. In contrast, the disrupted regions in the submodels of song2021 show a notable overlap when subjected to SRDA, consequently enabling a substantial number of pixels to remain vulnerable to ARDA. This phenomenon is consistent with the illustration in Fig. 10.

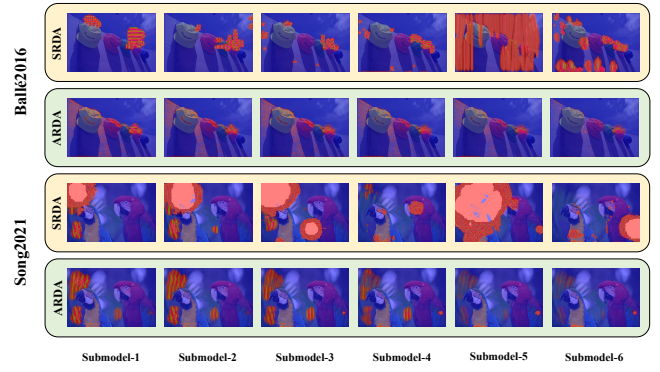


Fig. 11. Local attack effects on the reconstruction of Ballé2016 and Song2021, where the successfully attacked pixels and the failed attacked pixels are masked in red and blue respectively.

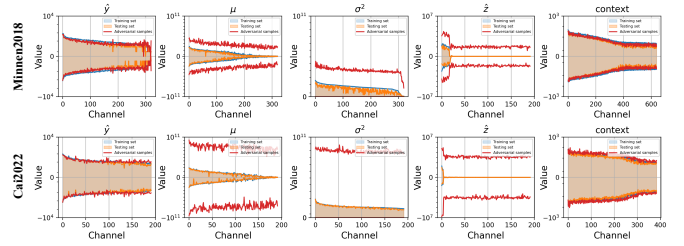


Fig. 12. Statistical analyses on latent features \hat{y} , mean μ and variance σ^2 of prior distributions, hyperprior \hat{z} , as well as the context information *context*.

D. Analysis on Latent Features

To deepen our understandings on the vulnerabilities of LIC algorithms against joint rate-distortion attacks, we conduct a statistical analysis on Minnen2018 and Cai2022, as shown in Fig. 12. It is evident that distortion vulnerabilities primarily come from minor perturbations on several feature channels, whereas rate vulnerabilities are present across all channels. The vulnerabilities of the prior distribution mainly come from the hyperprior \hat{z} . This explains why Ballé2016, which does not utilize hyperprior structure, maintains the best adversarial robustness in bitrate.

E. Effectiveness of Defense Techniques

In order to evaluate the efficacy of adversarial training and online updating in defending against joint rate-distortion

TABLE III
AVERAGED PERFORMANCE VARIATIONS (\downarrow) OVER ALL SUBMODELS AND ATTACK DIRECTIONS AFTER ADVERSARIAL TRAINING ON SRA, SDA, AND SRDA. THE WORST DEFENSE EFFECT AMONG THREE ATTACK METHODS IS HIGHLIGHTED IN RED.

Methods	SRA		SDA		SRDA	
	$\bar{\mu}(\Delta\mathcal{R})$	$\bar{\mu}(\Delta\mathcal{D})$	$\bar{\mu}(\Delta\mathcal{R})$	$\bar{\mu}(\Delta\mathcal{D})$	$\bar{\mu}(\Delta\mathcal{R})$	$\bar{\mu}(\Delta\mathcal{D})$
Ballé2016 [13]	0.1817	518.39	0.1934	129.75	0.1864	147.48
Ballé2018 [14]	0.3122	296.39	1.0912	86.67	0.3495	100.11
Minnen2018 [4]	0.3841	158.47	3.7523	76.29	0.5095	90.36
Cheng2020 [5]	0.2882	126.35	1.1138	88.38	0.2580	94.88
Song2021 [16]	0.4342	608.35	1.0251	1064.87	0.2876	99.42
Cai2022 [17]	0.2711	143.75	6.8692	257.62	0.3786	88.35
Zou2022 [6]	0.4064	130.15	2.6190	92.47	0.3798	91.75
Liu2023 [15]	0.3868	132.19	0.7491	94.32	0.3692	86.41

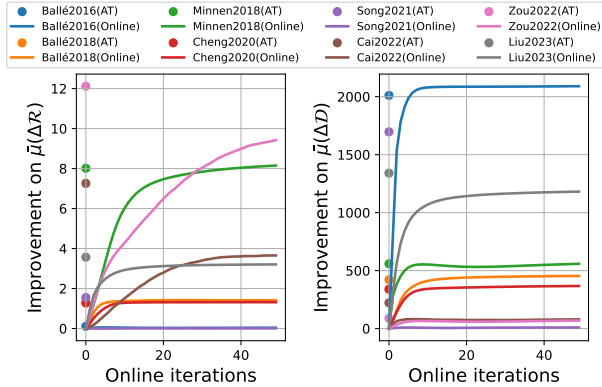


Fig. 13. Improvements on the adversarial robustness of adversarial training (AT) and online upadating (online).

attacks, we analyze their improvement on adversarial robustness within the context of SRDA, as shown in Fig. 13. The results demonstrate that adversarial training enhances the robustness of all LIC algorithms more effectively than online updating in general. While online updating shows slight better improvements over adversarial training in specific cases, such as reducing the bitrate of Minnen2018 and the distortion of Ballé2016. However, it performs poorly when applied to algorithms with more intricate structures like Song2021 and Liu2023. In addition, the efficiency of online updating on bitrate is lower than on distortion, this may be due to the higher deviation in bitrate-related features identified in the Fig. 12.

We further conduct experiments to investigate the efficacy of adversarial samples generated by singular dimensional attacks of either bitrate (SRA) or distortion (SDA), in adversarial training. The results presented in Tab. III reveal that, samples produced by singular dimensional attacks inadequately capture malicious disruptions in another dimension. This emphasizes the significance of the proposed joint rate-distortion attacks from a defensive perspective.

VIII. LIMITATIONS

This paper excludes the impact of other attack factors, such as variations in attack implementations and attack intensity. Instead, we concentrate on the attack direction and attack subject to investigate the intrinsic characteristics of adversarial robustness in LIC algorithms. Besides, we do not explore LIC methods with different reconstruction objectives, such as perceptual quality or downstream tasks. Nevertheless, we believe that our attack paradigms and analytical tools can facilitate the study of these algorithms. These aspects will be the main focus of our future research works.

IX. CONCLUSION

In this paper, we develop two attack paradigms for LIC algorithms to simulate real-world attacks at the submodel and algorithm levels. Additionally, we design a suite of multi-granularity assessment tools to evaluate the attack results. Through extensive experiments conducted on eight prominent

LIC methods, we derive a series of insights regarding the adversarial robustness from various perspectives. Furthermore, effectiveness of two defense techniques against joint rate-distortion attacks is explored. The experimental results can serve as valuable references for enhancing the development of compression algorithms with better adversarial robustness.

REFERENCES

- [1] G. K. Wallace, "The jpeg still picture compression standard," *IEEE Transactions on Consumer Electronics*, vol. 38, no. 1, pp. xviii–xxxiv, 1992.
- [2] G. J. Sullivan, J.-R. Ohm, W.-J. Han, and T. Wiegand, "Overview of the high efficiency video coding (hevc) standard," *IEEE Transactions on Circuits and Systems for Video Technology*, vol. 22, no. 12, pp. 1649–1668, 2012.
- [3] B. Bross, Y.-K. Wang, Y. Ye, S. Liu, J. Chen, G. J. Sullivan, and J.-R. Ohm, "Overview of the versatile video coding (vvc) standard and its applications," *IEEE Transactions on Circuits and Systems for Video Technology*, vol. 31, no. 10, pp. 3736–3764, 2021.
- [4] D. Minnen, J. Ballé, and G. D. Toderici, "Joint autoregressive and hierarchical priors for learned image compression," *Advances in Neural Information Processing Systems*, vol. 31, 2018.
- [5] Z. Cheng, H. Sun, M. Takeuchi, and J. Katto, "Learned image compression with discretized gaussian mixture likelihoods and attention modules," in *Proceedings of the IEEE/CVF Conference on Computer Vision and Pattern Recognition (CVPR)*, June 2020.
- [6] R. Zou, C. Song, and Z. Zhang, "The devil is in the details: Window-based attention for image compression," in *Proceedings of the IEEE/CVF Conference on Computer Vision and Pattern Recognition, 2022*, pp. 17 492–17 501.
- [7] N. Carlini, A. Athalye, N. Papernot, W. Brendel, J. Rauber, D. Tsipras, I. Goodfellow, A. Madry, and A. Kurakin, "On evaluating adversarial robustness," *arXiv preprint arXiv:1902.06705*, 2019.
- [8] T. Chen and Z. Ma, "Towards robust neural image compression: Adversarial attack and model finetuning," *IEEE Transactions on Circuits and Systems for Video Technology*, 2023.
- [9] Y. Sui, Z. Li, D. Ding, X. Pan, X. Xu, S. Liu, and Z. Chen, "Reconstruction distortion of learned image compression with imperceptible perturbations," in *ICML 2023 Workshop Neural Compression: From Information Theory to Applications*, 2023. [Online]. Available: <https://openreview.net/forum?id=38sgR7agFC>
- [10] K. Liu, D. Wu, Y. Wu, Y. Wang, D. Feng, B. Tan, and S. Garg, "Manipulation attacks on learned image compression," *IEEE Transactions on Artificial Intelligence*, 2023.
- [11] Z. Chen and K. N. Ngan, "Recent advances in rate control for video coding," *Signal Processing: Image Communication*, vol. 22, no. 1, pp. 19–38, 2007.
- [12] Y. Zhang, G. Lu, Y. Chen, S. Wang, Y. Shi, J. Wang, and L. Song, "Neural rate control for learned video compression," in *The Twelfth International Conference on Learning Representations*, 2023.
- [13] J. Ballé, V. Laparra, and E. P. Simoncelli, "End-to-end optimized image compression," in *5th International Conference on Learning Representations, ICLR 2017*, 2017.
- [14] J. Ballé, D. Minnen, S. Singh, S. J. Hwang, and N. Johnston, "Variational image compression with a scale hyperprior," in *International Conference on Learning Representations*.
- [15] J. Liu, H. Sun, and J. Katto, "Learned image compression with mixed transformer-cnn architectures," in *Proceedings of the IEEE/CVF Conference on Computer Vision and Pattern Recognition*, 2023, pp. 1–10.
- [16] M. Song, J. Choi, and B. Han, "Variable-rate deep image compression through spatially-adaptive feature transform," in *Proceedings of the IEEE/CVF International Conference on Computer Vision*, 2021, pp. 2380–2389.
- [17] S. Cai, Z. Zhang, L. Chen, L. Yan, S. Zhong, and X. Zou, "High-fidelity variable-rate image compression via invertible activation transformation," in *Proceedings of the 30th ACM International Conference on Multimedia*, 2022, pp. 2021–2031.
- [18] C. Szegedy, W. Zaremba, I. Sutskever, J. Bruna, D. Erhan, I. Goodfellow, and R. Fergus, "Intriguing properties of neural networks," in *2nd International Conference on Learning Representations, ICLR 2014*, 2014.
- [19] I. J. Goodfellow, J. Shlens, and C. Szegedy, "Explaining and harnessing adversarial examples," *arXiv preprint arXiv:1412.6572*, 2014.

- [20] A. Kurakin, I. Goodfellow, and S. Bengio, “Adversarial examples in the physical world. arxiv 2016,” *arXiv preprint arXiv:1607.02533*, 2016.
- [21] A. Madry, A. Makelov, L. Schmidt, D. Tsipras, and A. Vladu, “Towards deep learning models resistant to adversarial attacks,” *arXiv preprint arXiv:1706.06083*, 2017.
- [22] N. Carlini and D. Wagner, “Towards evaluating the robustness of neural networks,” in *2017 IEEE Symposium on Security and Privacy (SP)*. Ieee, 2017, pp. 39–57.
- [23] H. Xu, Y. Ma, H.-C. Liu, D. Deb, H. Liu, J.-L. Tang, and A. K. Jain, “Adversarial attacks and defenses in images, graphs and text: A review,” *International Journal of Automation and Computing*, vol. 17, pp. 151–178, 2020.
- [24] T. Bai, J. Luo, J. Zhao, B. Wen, and Q. Wang, “Recent advances in adversarial training for adversarial robustness,” *arXiv preprint arXiv:2102.01356*, 2021.
- [25] J. Campos, S. Meierhans, A. Djelouah, and C. Schroers, “Content adaptive optimization for neural image compression,” in *Proceedings of the IEEE/CVF Conference on Computer Vision and Pattern Recognition Workshops*, 2019, pp. 0–0.
- [26] J. Bégin, F. Racapé, S. Feltman, and A. Pushparaja, “Compressai: a pytorch library and evaluation platform for end-to-end compression research,” *arXiv preprint arXiv:2011.03029*, 2020.
- [27] R. Franzen, “True color kodak images,” <https://r0k.us/graphics/kodak/>, November 1999.

APPENDIX

A. Detailed Procedure of ARDA

Algorithm 2 Agnostic-ratio Rate-Distortion Attack (ARDA)

Input: Image $x \in \mathbb{R}^{H \times W \times C}$, attack coefficients γ_r and γ_d , maximum disturbance ϵ , attack steps \mathcal{T} on the surface of ϵ -sphere.

- 1: **Initialization:** $\delta = \vec{0}^{H \times W \times C}$
- 2: **repeat**
- 3: **while** $\|\delta\| > \epsilon$ **do**
- 4: $\arg \min_{\delta} \|\delta\|$
- 5: **end while**
- 6: **for** $k \in [1, N]$ **do**
- 7: Calculate $\mathcal{L}_s^{(k)}$ based on γ_r and γ_d . \triangleright Eq. (3)
- 8: Calculate $w^{(k)}$. \triangleright Eq. (5)
- 9: **end for**
- 10: Calculate \mathcal{L}_f based on $\mathcal{L}_s^{(k)}$ and $w^{(k)}$. \triangleright Eq. (4)
- 11: Update δ based on $\partial \mathcal{L}_f / \partial \delta$.
- 12: **until** \mathcal{T} attacks are made after the first reach of the ϵ -sphere surface

Output: $\max(\min(x_a, 1), 0)$

B. RD Performance Under ARDA

RD performance of compression methods under various directions of ARDA is shown in Fig. 16. The compression algorithms show similar robustness across various bitrates, except for variable-rate methods Song2021 and Cai2022. High bitrates of variable-rate methods are found to be more vulnerable to ARDA, especially under rate-oriented attacks. This could be due to the consistent weakness among submodels and more reservation of malicious information in high bitrates.

C. More Experiments on Defense Techniques

1) *Defensing Against ARDA:* Similar to Fig. 13, we present the improvement of two defense techniques on adversarial

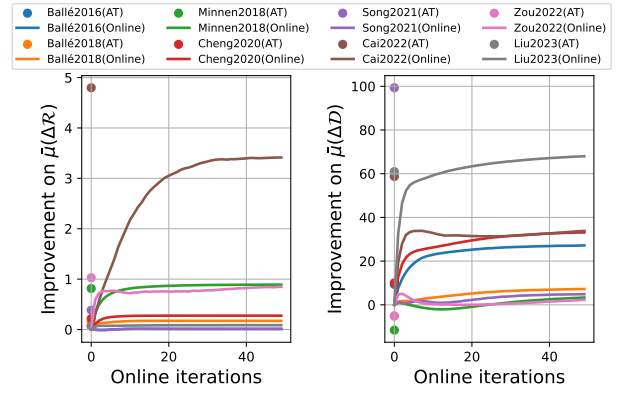


Fig. 14. Improvements of defense techniques on the adversarial robustness against ARDA.

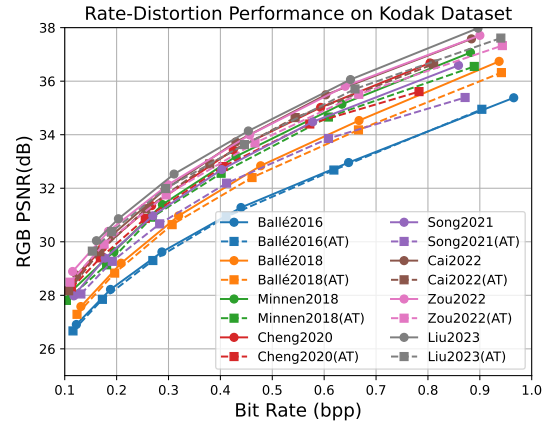


Fig. 15. RD performance before and after AT on Kodak dataset.

robustness against ARDA in Fig. 14. In comparison to the inferior performance relative to adversarial training under SRDA, online updating under ARDA shows a noticeable improvement. However, it still exhibits poor performance when applied to variable-rate methods Song2021 and Cai2022. This limitation may come from the instability of these methods during optimization, which is caused by training for multiple bitrate targets.

2) *RD Performance on Clean Images After AT:* AT changes the model parameters of compression algorithms by finetuning on adversarial samples. We present the variation of RD performance on the original Kodak dataset in Fig. 15. It is found that the performance exhibits a small degree of degradation after AT. It is acceptable when compared to the significant improvement on the robustness against malicious disturbance.

3) *Combination of AT and Online:* The two defense techniques discussed in the main paper operate during the training and testing phase, respectively. We conduct experiments to evaluate the combined defending effects against SRDA, as depicted in Fig. 17. It is observed that performing online updating on the basis of adversarial training can further improve the distortion, but it will compromise the bitrate of some algorithms.

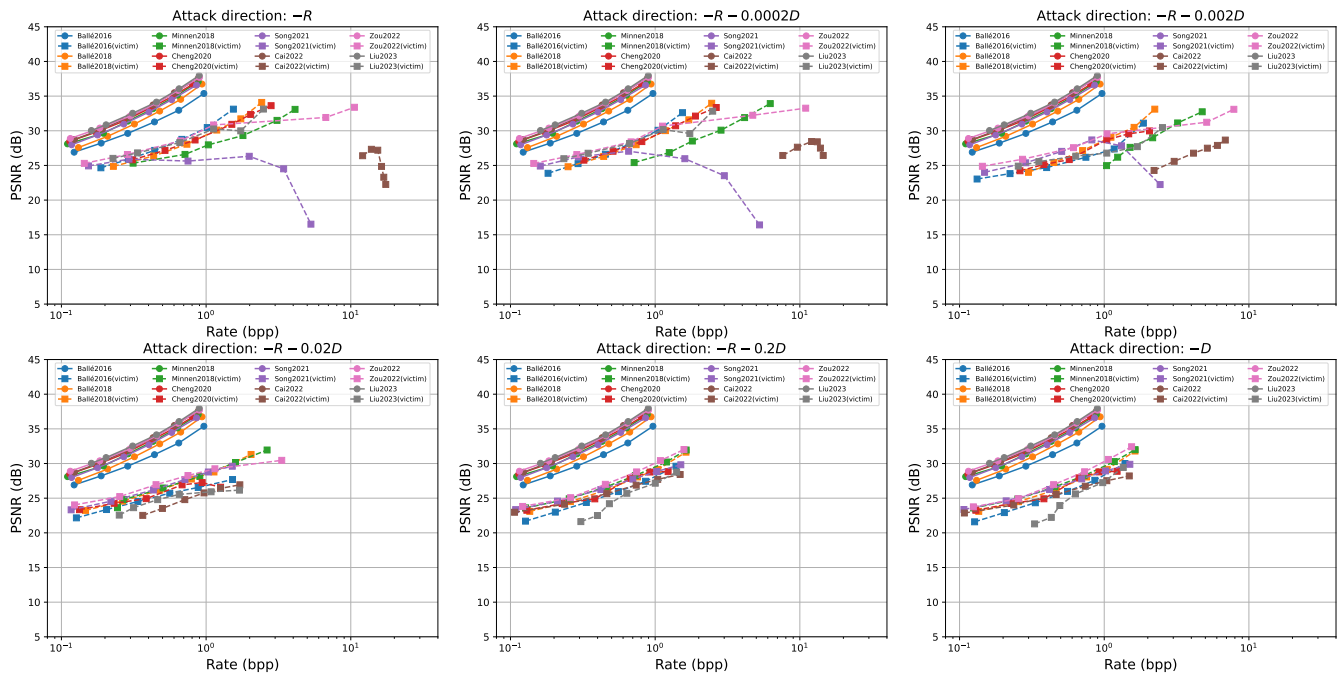


Fig. 16. RD performance under six attack directions of ARDA. The performance of the same compression algorithm before and after an attack is depicted using solid and dashed lines in the same color.

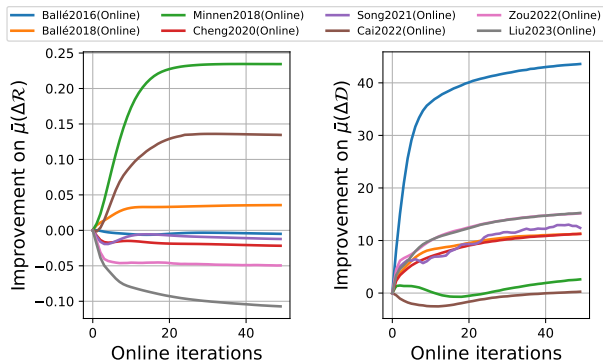


Fig. 17. The effect of the combination of two defense techniques against SRDA.

D. More Statistical Analysis

As a supplement to Fig. 12, the feature ranges of the remaining six algorithms are visualized in Fig. 18. The features that do not exist in the corresponding algorithm are omitted. In the channel context methods Zou2020 and Liu2023, contextual information is not explicitly extracted, thus is also omitted in the figure. The statistical analysis reveals a significant correlation in the variations of features across different compression methods. This universal characteristic can help to improve defense techniques against adversarial attacks.

E. Visualization of Attack Effect

To demonstrate the vulnerability of the LIC algorithm to malicious attacks, we present more compression results of different attack directions and different submodels. Results under SRDA and ARDA are presented in Figs. 19, 20 and Figs.

21, 22, respectively. Under adversarial attacks, invalid values (NaN) are easy to appear in the reconstruction of Song2021, we replace these values with 255. In comparison to SRDA, the attack effect under ARDA is subtle in thumbnail view. For convenience, we highlight the corruption under ARDA with a red box.

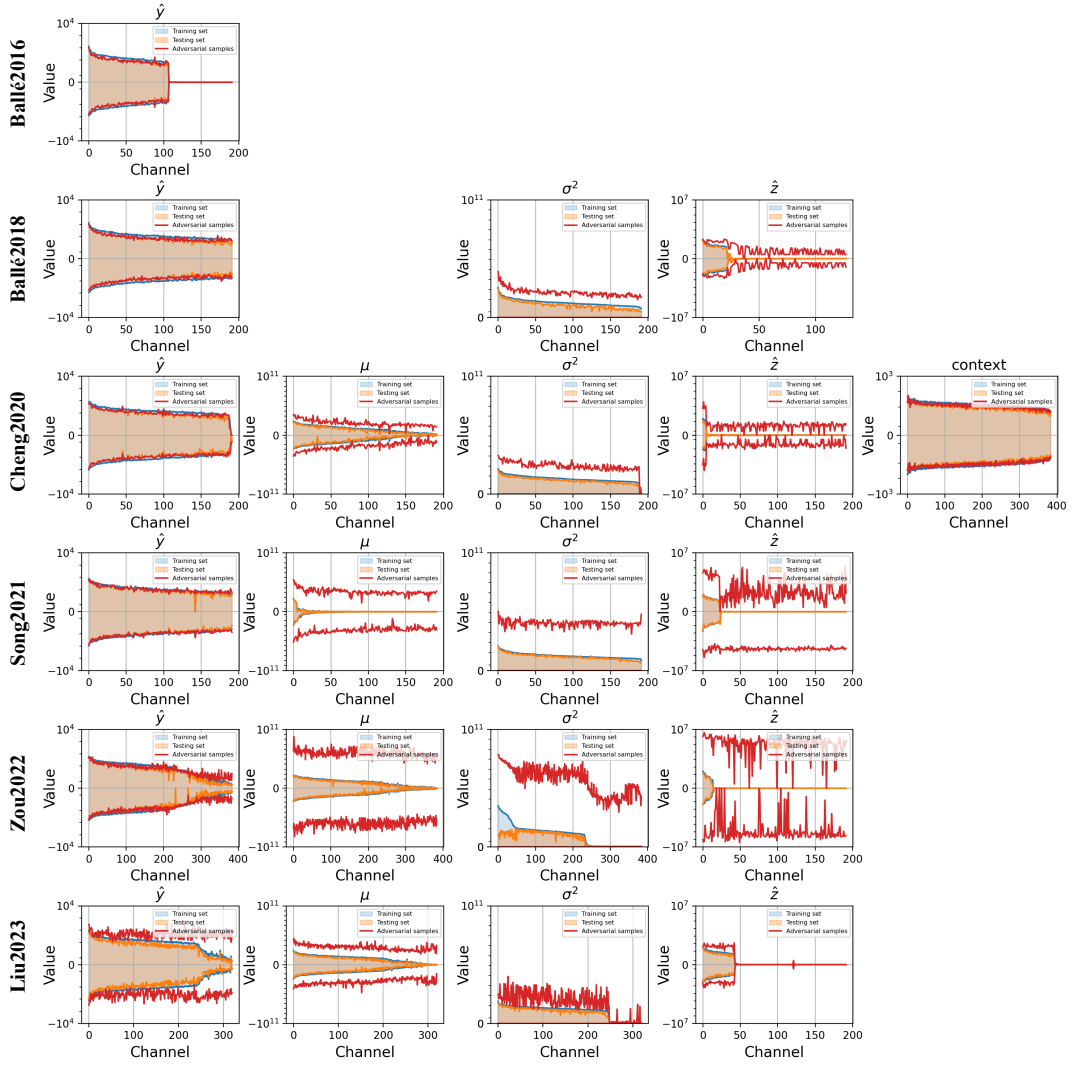


Fig. 18. Statistical analysis on latent features \hat{y} , mean μ and variance σ^2 of prior distributions, hyperprior \hat{z} , as well as the context information *context*.



Fig. 19. Bitrate and reconstruction of submodel-5 in experimental algorithms under different attack directions of SRDA.













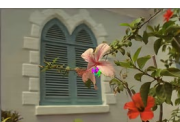
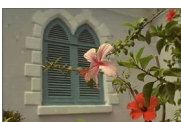
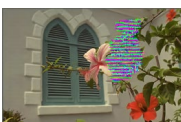
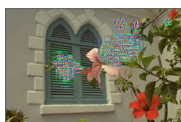
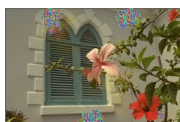
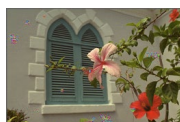

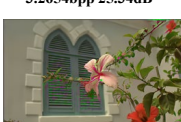

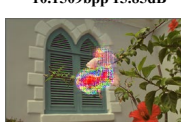
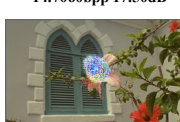
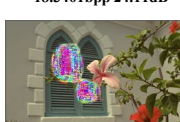
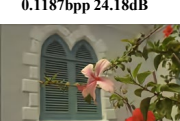

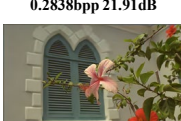
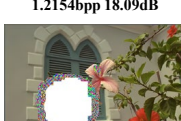



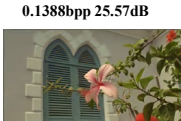
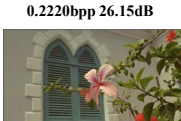



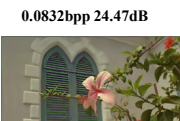


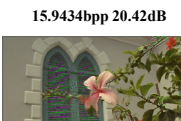
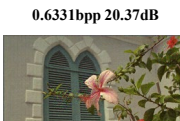
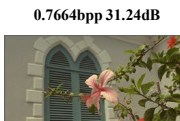
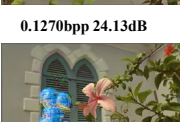
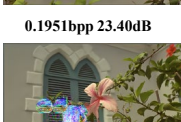
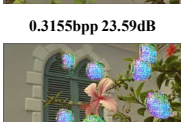

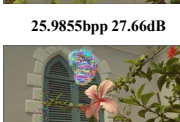
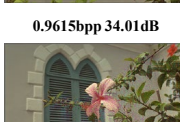
	Submodel-1	Submodel-2	Submodel-3	Submodel-4	Submodel-5	Submodel-6
Balle2016	 0.1318bpp 15.72dB	 0.1926bpp 16.07dB	 0.2863bpp 17.32dB	 0.4320bpp 14.34dB	 0.7593bpp 8.17dB	 0.9560bpp 14.37dB
Balle2018	 0.1311bpp 22.13dB	 0.2309bpp 17.69dB	 0.3072bpp 22.08dB	 0.4629bpp 17.37dB	 0.6571bpp 14.47dB	 5.9097bpp 19.75dB
Minnen2018	 0.1147bpp 24.27dB	 3.2654bpp 25.34dB	 1.9951bpp 16.32dB	 10.1509bpp 15.85dB	 14.7060bpp 17.50dB	 18.3401bpp 24.11dB
Cheng2020	 0.1187bpp 24.18dB	 0.1841bpp 23.68dB	 0.2838bpp 21.91dB	 1.2154bpp 18.09dB	 0.4926bpp 20.44dB	 0.6901bpp 16.25dB
Song2021	 0.1087bpp 23.61dB	 0.1388bpp 25.57dB	 0.2220bpp 26.15dB	 1.4584bpp 12.35dB	 13.3146bpp 6.17dB	 2.2061bpp 12.85dB
Cai2022	 0.0832bpp 24.47dB	 0.1209bpp 25.05dB	 0.1945bpp 25.63dB	 15.9434bpp 20.42dB	 0.6331bpp 20.37dB	 0.7664bpp 31.24dB
Zou2022	 0.1270bpp 24.13dB	 0.1951bpp 23.40dB	 0.3155bpp 23.59dB	 0.9438bpp 22.15dB	 25.9855bpp 27.66dB	 0.9615bpp 34.01dB
Lin2023	 0.5434bpp 16.41dB	 0.9955bpp 17.18dB	 2.8163bpp 13.86dB	 0.5897bpp 20.38dB	 1.3530bpp 18.50dB	 2.0423bpp 19.35dB

Fig. 20. Bitrate and reconstruction of six submodels in experimental algorithms under attack direction $-\mathcal{R} - 0.02\mathcal{D}$ of SRDA.

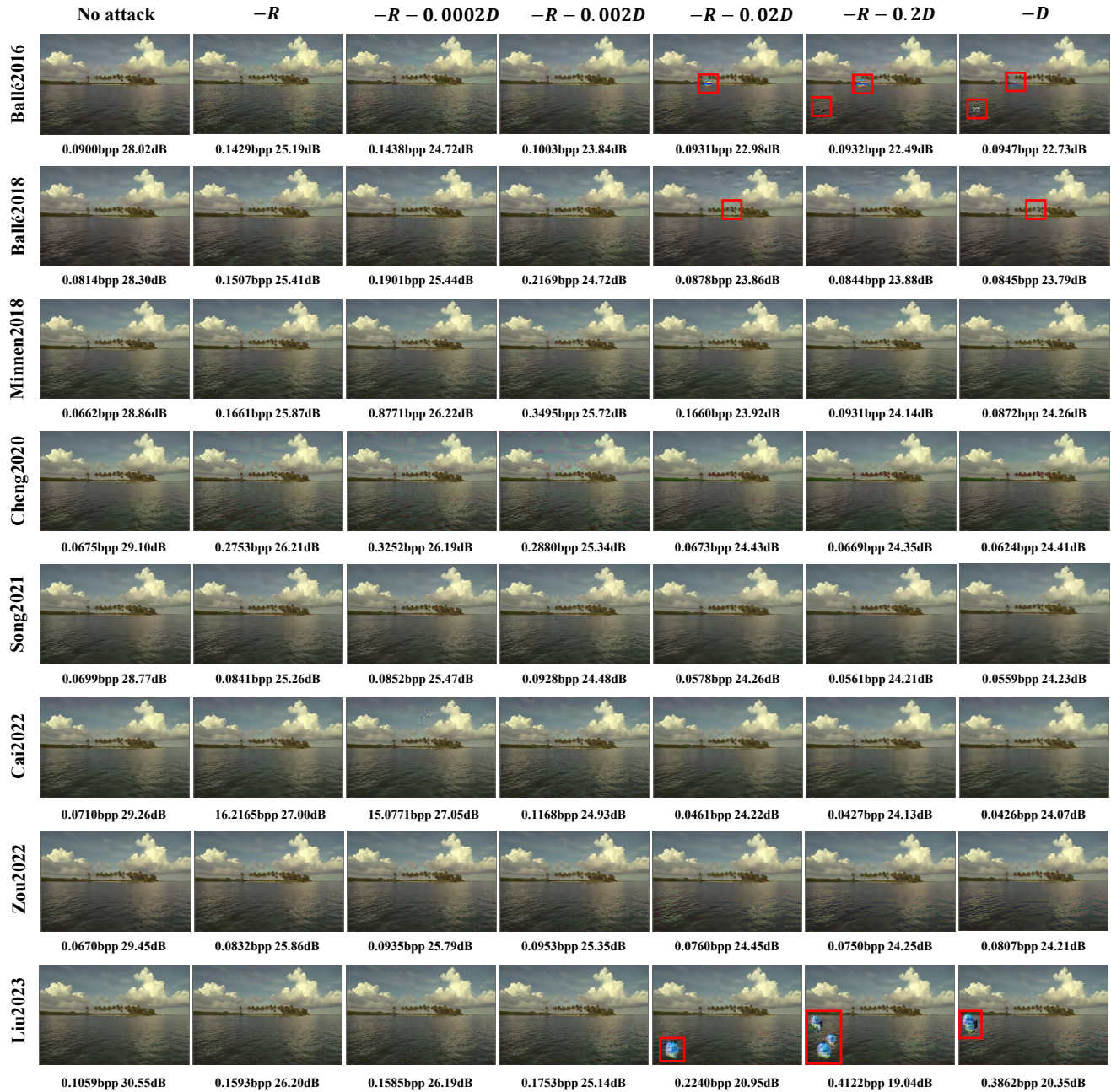


Fig. 21. Bitrate and reconstruction of submodel-1 in experimental algorithms under different attack directions of ARDA.

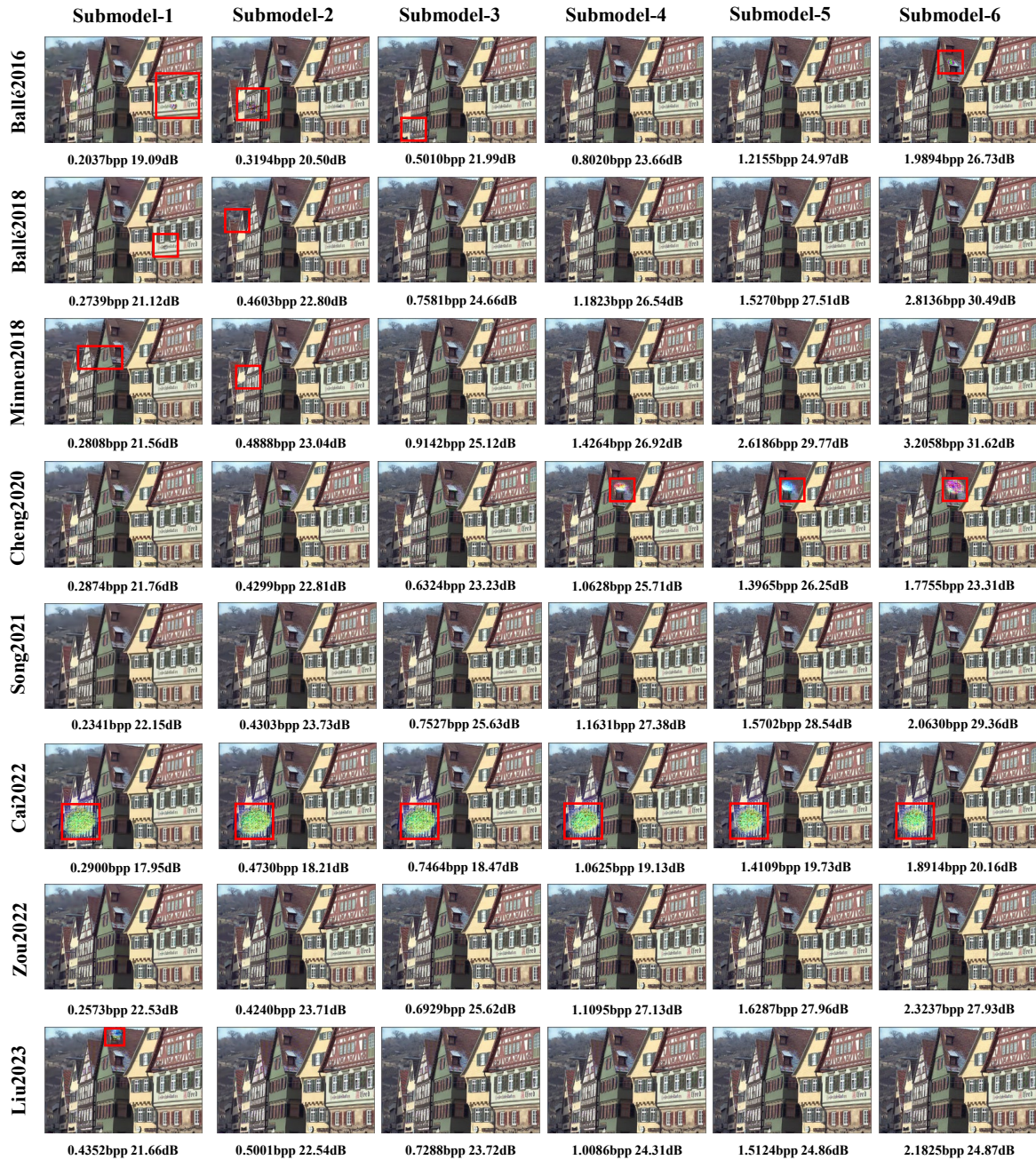


Fig. 22. Bitrate and reconstruction of six submodels in experimental algorithms under attack direction $-\mathcal{R} - 0.02D$ of ARDA.